Functional Interactions Between *SPO11* and *REC102* During Initiation of Meiotic Recombination in *Saccharomyces cerevisiae*

Kehkooi Kee and Scott Keeney[1]

Molecular Biology Program, Memorial Sloan-Kettering Cancer Center and Weill Graduate School of Medical Sciences of Cornell University, New York, New York 10021

Manuscript received March 20, 2001
Accepted for publication October 31, 2001

ABSTRACT

In *Saccharomyces cerevisiae*, formation of the DNA double-strand breaks (DSBs) that initiate meiotic recombination requires the products of at least 10 genes. Spo11p is thought to be the catalytic subunit of the DNA cleaving activity, but the roles of the other proteins, and the interactions among them, are not well understood. This study demonstrates genetic and physical interactions between the products of *SPO11* and another early meiotic gene required for DSB formation, *REC102*. We found that epitope-tagged versions of *SPO11* and *REC102* that by themselves were capable of supporting normal or nearly normal levels of meiotic recombination conferred a severe synthetic cold-sensitive phenotype when combined in the same cells. DSB formation, meiotic gene conversion, and spore viability were drastically reduced in the doubly tagged strain at a nonpermissive temperature. This conditional defect could be partially rescued by expression of untagged *SPO11*, but not by expression of untagged *REC102*, indicating that tagged *REC102* is fully dominant for this synthetic phenotype. Both tagged and wild-type Spo11p co-immunoprecipitated with tagged Rec102p from meiotic cell extracts, indicating that these proteins are present in a common complex *in vivo*. Tagged Rec102p localized to the nucleus in whole cells and to chromatin on spread meiotic chromosomes. Our results are consistent with the idea that a multiprotein complex that includes Spo11p and Rec102p promotes meiotic DSB formation.

IN most sexually reproducing organisms, homologous recombination plays a key role in accurate chromosome segregation at the first meiotic division (Moore and Orr-Weaver 1998). Recent studies are providing insight into the molecular mechanisms underlying meiotic recombination in several organisms, but the process is best understood in *Saccharomyces cerevisiae*. Meiotic recombination in budding yeast proceeds via the formation and subsequent repair of DNA double-strand breaks (DSBs; Smith and Nicolas 1998; Keeney 2001). A large number of genes are required for DSB formation, of which several are expressed in meiotic cells only. These include *SPO11*, *MEI4*, *MER2*, *REC102*, *REC104*, and *REC114* (Keeney 2001). Three others also play roles in mitotic DNA metabolism: *MRE11*, *RAD50*, and *XRS2* (Haber 1998; Paques and Haber 1999). Null mutants for any of these genes fail to carry out meiotic recombination and show wholesale chromosome nondisjunction at meiosis I, giving rise to inviable, aneuploid spores.

SPO11 was one of the first meiotic recombination genes identified (Esposito and Esposito 1969; Klapholz *et al.* 1985). Its product is thought to be the catalytic subunit of the meiotic DSB-forming activity, cleaving DNA via a topoisomerase-like transesterification reaction (Bergerat *et al.* 1997; Keeney *et al.* 1997). Homologs of Spo11p are required for meiotic recombination in *Schizosaccharomyces pombe*, the basidiomycete *Coprinus cinereus*, *Caenorhabditis elegans*, *Drosophila melanogaster*, *Arabidopsis thaliana*, and mouse (Lin and Smith 1994; Dernburg *et al.* 1998; McKim and Hayashi-Hagihara 1998; Baudat *et al.* 2000; Celerin *et al.* 2000; Romanienko and Camerini-Otero 2000; Grelon *et al.* 2001; Mahadevaiah *et al.* 2001). Thus, it appears that the roles of Spo11p and DSB formation in meiotic recombination are evolutionarily conserved.

Less is known about the roles of the other meiosis-specific yeast gene products required for DSB formation. *REC102* was identified in a screen for mutations that rescued the meiotic lethality in a *rad52 spo13* haploid strain (Malone *et al.* 1991) and independently as a mutation that produced inviable spores (Bhargava *et al.* 1992). Mutations in *REC102* cause defects in DSB formation and meiotic recombination, but have no effect on mitotic recombination frequency (Bhargava *et al.* 1992; Cool and Malone 1992; Bullard *et al.* 1996). The mutants form axial elements but, like *spo11* mutants, are defective for formation of tripartite synaptonemal complex (Giroux *et al.* 1989; Bhargava *et al.* 1992; Loidl *et al.* 1994). Also like *spo11* mutants, *rec102* null mutants appear to enter the meiosis I division earlier than normal in at least some strain backgrounds (Jiao *et al.* 1999). *REC102* mRNA is expressed only in meiosis and encodes a predicted pro-

[1]*Corresponding author:* Memorial Sloan-Kettering Cancer Center, 1275 York Ave., Box 97, New York, NY 10021.
E-mail: s-keeney@ski.mskcc.org

tein product of 23 kD containing a putative leucine zipper, but with no other motifs to suggest a biochemical function (Cool and Malone 1992). No *REC102* homologs have been described in species other than hemiascomycetes. Recently, overexpression of *REC102* was found to suppress the recombination defects conferred by temperature-sensitive *rec104* alleles, demonstrating a genetic interaction between *REC102* and *REC104* (Salem *et al.* 1999).

For Rec102p (and other DSB proteins) to have a role in DSB formation, it must exert its influence on the activity of Spo11p itself. But whether this influence is a result of direct interactions with Spo11p or of indirect connections (such as by regulating gene expression) is not known. Here, we describe evidence for genetic and physical interactions between Rec102p and Spo11p that supports the idea that these proteins are components of a multiprotein complex responsible for initiating meiotic recombination.

MATERIALS AND METHODS

Yeast strains and plasmids: The yeast strains and plasmids used in this study are listed in Table 1. All strains are isogenic diploid derivatives of SK1 (Kane and Roth 1974) and were derived from strains originally provided by N. Kleckner, Harvard University. Yeast transformations were performed using the lithium acetate/polyethylene glycol method (Gietz and Woods 1998). The *REC102-myc9::URA3* allele was constructed by the "megaprimer" method (Ke and Madison 1997) as follows: A 343-bp fragment from the 3′ end of the *REC102* coding sequence and a 626-bp fragment extending into the 3′ untranslated region were amplified by PCR from SK1 genomic DNA and were cloned into the *URA3* integrating vector pRS306 (Sikorski and Hieter 1989) and the sequence was verified. The PCR primers were designed to introduce a unique *Spe*I site immediately prior to the stop codon; a 366-bp fragment encoding nine repeats of the myc epitope (EQKLISEEDL; provided by K. Nasmyth, University of Vienna) was inserted into this *Spe*I site. The resulting plasmid (pKK2) was linearized with *Mun*I and used to transform strain NKY611 to Ura+. Correct integration at the endogenous *REC102* locus resulted in a tandem array comprising full-length *REC102-myc9* under the control of the normal *REC102* promoter, *URA3* within pRS306 vector sequences, and an untagged, 0.55-kb, 3′ *rec102* fragment without a promoter. This structure was verified by PCR and by Southern blotting of genomic DNA. *REC102-myc9::TRP1* was generated by subcloning the 3′-*REC102-myc9* construct from pKK2 into pRS304 (Sikorski and Hieter 1989) and linearizing the resulting plasmid (pKK10) with *Ppu*MI for integration. The *REC102-Flag3::TRP1* allele was created by inserting a 321-bp fragment from the 3′ end of *REC102* into pRS304-3Flag (Green *et al.* 2000; provided by N. Lowndes, Imperial Cancer Research Fund). The resulting plasmid (pKK15) was integrated into the genome after linearization with *Ppu*MI.

The *SPO11* allele with a single hemagglutinin (HA) tag used in this study was described previously (Keeney *et al.* 1997). To construct *spo11-HA3His6::kanMX4*, we started with a version of *SPO11* with a 3′ in-frame fusion to a *Xho*I site and an 18-bp sequence encoding six histidines, constructed as described for single-HA-tagged *SPO11* (Keeney *et al.* 1997) and generously provided by C. Giroux, Wayne State University, Detroit. This *SPO11-His6* construct, also carrying 422 bp of upstream and 400 bp of downstream genomic sequences, was subcloned into pRS306, and then a 112-bp cassette encoding three repeats of the HA1 epitope (Tyers *et al.* 1992), YPYDVPDYA, was inserted into the *Xho*I site to generate pSK52. The *kanMX4* G418-resistance cassette (Wach *et al.* 1998) was inserted into the unique *Swa*I site in the intergenic region downstream of *spo11-HA3His6* to generate pSK54. Transcription of the *kanMX4* cassette is in the same direction as *spo11-HA3His6*. We replaced the 3′ end of the endogenous *SPO11* gene with this construct by transforming cells with a 2.2-kbp *Eco*RI to *Sac*II restriction fragment from pSK54, encompassing the 3′-most 337 bp of the *spo11-HA3His6* coding sequence, 400 bp of downstream genomic sequence, and the inserted *kanMX4* cassette. Correct integration was confirmed by PCR and Southern blotting of genomic DNA. The *spo11-HA3His6* allele is indicated in lowercase to reflect the recessivity of its cold-sensitive defect (see below).

Culture methods: For spore viability tests, cells were sporulated at the indicated temperature in liquid sporulation medium (SPM; 0.3% potassium acetate, 0.02% raffinose) or on plates (SPM plus 2% Bacto agar), and tetrads were dissected on YPD plates (1% yeast extract, 2% Bacto Peptone, 2% glucose, 2% agar). Spores were allowed to germinate and grow at 30°. The statistical significance of observed differences in spore viabilities was assessed by *z*-test, using a Microsoft Excel spreadsheet calculator written by M. F. F. Abdullah, Oxford University. Synchronous meiotic cultures were prepared as described previously (Alani *et al.* 1990; Padmore *et al.* 1991). Briefly, yeast cells were pregrown in liquid YPA (1% yeast extract, 2% Bacto Peptone, 1% potassium acetate) for 13.5 hr at 30°. Cells were harvested, washed, and then resuspended in SPM preequilibrated at the indicated temperature.

Meiosis I nuclear division profiles: Aliquots were collected at various times from synchronized meiotic cultures and adjusted to 50% (v/v) ethanol and 0.1 μg/ml 4′,6-diamidino-2-phenylindole (DAPI). Mononucleate, binucleate, and tetranucleate cells were scored by epifluorescence microscopy of at least 100 cells per time point.

Meiotic recombination assay: The frequency of meiotic recombination was determined by a "return-to-growth" assay (Sherman and Roman 1963). Strains with *his4::LEU2* heteroalleles (Cao *et al.* 1990) were pregrown in YPA at 30° and then transferred to SPM. Cultures were divided and incubated at 30° or 16°. Samples were collected at 0 hr and at either 8 hr (30° culture) or 13 hr (16° culture), sonicated, diluted in distilled water, and plated on YPD to measure total viable cells and on synthetic growth medium lacking histidine to measure prototroph formation. Colonies were scored after 2–3 days at 30°. For the 16° cultures, plates were preequilibrated at 16° prior to spreading and were incubated overnight at 16° after spreading before being shifted to 30°.

DSB analysis: Genomic DNA was purified from cells collected from synchronized cultures as described (Cao *et al.* 1990; Bishop *et al.* 1992). DNA was digested with *Eco*RI, electrophoresed on 0.8% agarose gels in 1× TBE, and blotted by capillary transfer to Hybond N+ membranes (Amersham, Piscataway, NJ). DSBs at the hotspot between open reading frames (ORFs) YCR047c and YCR048w (*ARE1*; Goldway *et al.* 1993; Baudat and Nicolas 1997) were detected with a ^{32}P-labeled 0.87-kb *Pst*I fragment spanning the 5′ region of *THR4* as described (Keeney and Kleckner 1995). Blots were visualized by autoradiography and quantitated with a FUJI BAS-2500 phosphorimager system.

Immunoprecipitation and Western analysis: Immunoprecipitations in which both Spo11p and Rec102p were epitope tagged were performed as follows. Approximately 2×10^9 cells were collected from synchronized meiotic cultures and lysed by agitation with glass beads in IP dilution buffer (0.01% SDS, 1.1% Triton X-100, 1.2 mm EDTA, 16.7 mm Tris-HCl, pH 8.1, 167 mm NaCl, containing the following protease inhibitors: 0.4 mm pefabloc-SC; 1 mm ε-aminocaproic acid; 1 mm *p*-aminobenzamidine; 1 mm phenylmethylsulfonylfluoride; and 1 μg/ml

TABLE 1

Yeast strains and plasmids

Strain	Genotype[a]
NKY611	*MAT***a** *ho::LYS2 ura3 lys2 leu2::hisG* *MAT*α *ho::LYS2 ura3 lys2 leu2::hisG*
SKY10	*his4X::LEU2 spo11Δ::hisG-URA3-hisG* *his4B::LEU2 spo11Δ::hisG-URA3-hisG*
SKY212	*REC102-myc9::URA3* *REC102-myc9::URA3*
SKY223	*spo11-HA3His6::kanMX4* *spo11-HA3His6::kanMX4*
SKY291	*spo11-HA3His6::kanMX4 REC102-myc9::URA3* *spo11-HA3His6::kanMX4 REC102-myc9::URA3*
SKY284	*spo11-HA3His6::kanMX4 REC102-myc9::URA3* *SPO11 REC102*
SKY348	*spo11-HA3His6::kanMX4 REC102-myc9::URA3* *spo11-HA3His6::kanMX4 REC102*
SKY470	*trp1::hisG arg4-Bgl his4B::LEU2 spo11-HA3His6::kanMX4 REC102-myc9::TRP1* *trp1::hisG arg4-Nsp his4X::LEU2 spo11-HA3His6::kanMX4 REC102-myc9::TRP1*
SKY490	*trp1::hisG arg4-Bgl his4B::LEU2* *trp1::hisG arg4-Nsp his4X::LEU2*
SKY493	*trp1::hisG arg4-Bgl his4B::LEU2 REC102-myc9::URA3* *trp1::hisG arg4-Nsp his4X::LEU2 REC102-myc9::URA3*
SKY496	*trp1::hisG arg4-Bgl his4B::LEU2 spo11-HA3His6::kanMX4* *trp1::hisG arg4-Nsp his4X::LEU2 spo11-HA3His6::kanMX4*
SKY501	*SPO11-HA::kanMX4* *SPO11-HA::kanMX4*
SKY540	*spo11-HA3His6::kanMX4 REC102-myc9::URA3* *SPO11 REC102-myc9::URA3*
SKY568	*trp1::hisG arg4-Bgl his4B::LEU2 REC102-Flag3::TRP1* *trp1::hisG arg4-Nsp his4X::LEU2 REC102-Flag3::TRP1*
SKY571	*arg4-Bgl his4B::LEU2 REC102-Flag3::TRP1 spo11-HA3His6::kanMX4* *arg4-Nsp his4X::LEU2 REC102-Flag3::TRP1 spo11-HA3His6::kanMX4*

Plasmid	Content
pKK2	pRS306 carrying 3′-*rec102-myc9*
pKK5	pRS315 (*LEU2 ARS/CEN* vector) carrying wild-type *SPO11*
pKK6	pRS315 carrying *spo11-HA3His6*
pKK9	pRS315 carrying wild-type *REC102*
pKK10	pRS304 (*TRP1* integration vector) carrying 3′-*rec102-myc9*
pKK11	pRS426 (2μ *URA3* vector) carrying wild-type *REC102*
pKK15	pRS304 carrying 3′-*rec102-Flag3*
pRS304-3flag	pRS304 carrying 3 repeats of the Flag epitope
pSK54	pRS306 with *spo11-HA3His6::kanMX4*

[a] All strains are *MAT***a**/*MAT*α and homozygous for *ho::LYS2*, *lys2*, *ura3*, and *leu2::hisG*. Strains NKY611 and SKY10 (also known as NKY2967) were provided by N. Kleckner; all other strains were derived in this study.

each of leupeptin, pepstatin A, and chymostatin). The lysates were centrifuged twice for 10 min at 16,000 × *g*, 4°. The supernatant was collected, adjusted to 10 mM $MgCl_2$, and then treated with 20 μg/ml DNase I for 30 min at room temperature. One milliliter of the extract was added to 0.5 ml of anti-myc affinity matrix (monoclonal 9E10 immobilized on Sepharose; BAbCo) and incubated 3 hr at the same temperature used for the meiotic culture. The supernatant was collected and the matrix was washed with 15 ml of IP dilution buffer. Bound proteins were eluted twice for 15 min with 1.5 ml 0.1 M glycine, pH

TABLE 2

Synthetic cold sensitivity associated with epitope tagging *REC102* and *SPO11*

Strain	Relevant genotype	Sporulation temp.:	% viable spores[a]			
			16°	23°	30°	37°
NKY611	Wild type		96 (20)	100 (20)	93 (20)	93 (20)
SKY212	*REC102-myc9* / *REC102-myc9*		98 (21)	95 (20)	97 (15)	92 (8)
SKY501	*SPO11-HA* / *SPO11-HA*		98 (20)	ND[b]	98 (20)	ND[b]
SKY223	*spo11-HA3His6* / *spo11-HA3His6*		59 (19)	ND[b]	97 (26)	90 (5)
SKY291	*REC102-myc9* / *REC102-myc9*, *spo11-HA3His6* / *spo11-HA3His6*		<1[c] (24)	7 (64)	78 (30)	73 (17)
SKY568	*REC102-Flag3* / *REC102-Flag3*		98 (20)	ND[b]	99 (20)	ND[b]
SKY571	*REC102-Flag3* / *REC102-Flag3*, *spo11-HA3His6* / *spo11-HA3His6*		<0.5[c] (50)	ND[b]	94 (35)	ND[b]

[a] The numbers of four-spored asci dissected are indicated in parentheses.
[b] ND, not determined.
[c] No viable spores were recovered.

2.9, and then TCA-precipitated and dissolved in 50 μl SDS sample buffer. Immunoprecipitations with anti-Flag antibody M2 (Sigma, St. Louis) were performed in essentially the same manner, except that bound proteins were eluted by competition with synthetic Flag peptide, and the eluates were concentrated by ultrafiltration.

For immunoprecipitations in which only Rec102p was tagged, an extract enriched for chromatin-associated proteins was prepared as follows. Approximately 3×10^{10} meiotic cells were collected and spheroplasts were prepared by digestion with zymolyase. Spheroplasts were lysed with 10 strokes in a Dounce homogenizer in 5 volumes of HLB (100 mM MES-NaOH, pH 6.4, 1 mM EDTA, 0.5 mM $MgCl_2$, plus protease inhibitors as above), then a crude nuclear fraction was obtained by centrifugation through a 30% glucose cushion in HLB. The pellet was extracted with 1 volume of EBX buffer (50 mM HEPES-NaOH, pH 7.5, 100 mM KCl, 2.5 mM $MgCl_2$, 0.05% Triton X-100, plus protease inhibitors) and recentrifuged at 14,000 × *g* for 10 min. The pellet was resuspended in one-third the original volume of EBX, then $MgCl_2$ and DNase I were added to final concentrations of 4.5 mM and 10 units/ml, respectively. This suspension was incubated on ice for at least 2 hr and then centrifuged at 14,000 × *g* for 10 min. The supernatant was subjected to immunoprecipitation with anti-myc antibodies as described above.

A portion of the immunoprecipitated material was subjected to 10% SDS-PAGE and blotted to Immobilon-P in 10 mM CAPS-NaOH, pH 11, 10% methanol. Blots were probed with anti-myc (9E10; BAbCo), anti-Flag (M2; Sigma), anti-HA (F-7; Santa Cruz Biotechnology), or an affinity-purified rabbit polyclonal antibody raised against recombinant Spo11 protein, and then with sheep anti-mouse or anti-rabbit IgG conjugated to horseradish peroxidase (Amersham). Chemiluminescent detection was performed according to the manufacturer's instructions (ECL+; Amersham). For analysis of steady-state protein levels, whole-cell protein extracts were prepared from 2 OD_{600} units of cells lysed with glass beads in SDS sample buffer essentially as described (Kaiser *et al.* 1994).

Indirect immunofluorescence: Nuclear spreads were prepared according to previously described methods (Loidl *et al.* 1991, 1998). Whole cells were prepared for staining as described (Pringle *et al.* 1991), except that cells were fixed with formaldehyde for 15 min and cell walls were partially digested by 5 min incubation at 30° in 50 μg/ml zymolyase 100T in ZK buffer (0.4 M sorbitol, 0.4 M KCl, 40 mM K_2HPO_4, 0.5 mM $MgCl_2$). Indirect immunofluorescent staining was carried out as described (Gasior *et al.* 1998). Anti-myc primary antibody 9E10 (BAbCo) was used at a 1:500 dilution. Goat anti-mouse IgG coupled to Alexa 488 (Molecular Probes, Eugene, OR) was used at a 1:1000 dilution. Slides were mounted with cover slips in Prolong antifade (Molecular Probes) containing 50 ng/ml DAPI. Images were captured on a Zeiss Axiophot microscope with a 100× objective using a Cooke Sensicam cooled CCD camera. Data capture and image processing were performed using the Slidebook software package (Intelligent Imaging Innovations).

RESULTS

Synthetic defects in meiotic recombination caused by epitope tagging Rec102p and Spo11p: As part of studies of the roles of Spo11p and Rec102p in meiotic recombination, we generated affinity-tagged versions of each protein. Rec102p was tagged at its carboxyl terminus with nine repeats of the myc epitope (Rec102-myc9p), and Spo11p was tagged at its carboxyl terminus with three repeats of the HA epitope plus a hexahistidine sequence (Spo11-HA3 His6p). Each was integrated into the genome at its respective locus and expressed under the control of its own promoter. When sporulated at 30°, diploid strains homozy-

TABLE 3

Rescue of the synthetic cold-sensitive defect by *SPO11* but not by *REC102*

Strain	Relevant genotype	Plasmid	% viable spores produced at 16°[a]
SKY291	*REC102-myc9*/*REC102-myc9*, *spo11-HA3His6*/*spo11-HA3His6*	pKK5 (*SPO11*)	71 (33)
SKY291	*REC102-myc9*/*REC102-myc9*, *spo11-HA3His6*/*spo11-HA3His6*	pKK6 (*spo11-HA3His6*)	<0.7[b] (35)
SKY540	*REC102-myc9*/*REC102-myc9*, *spo11-HA3His6*/+	—	98 (40)
SKY291	*REC102-myc9*/*REC102-myc9*, *spo11-HA3His6*/*spo11-HA3His6*	pKK9 (*REC102*)	<0.9[b] (27)
SKY470	*REC102-myc9*/*REC102-myc9*, *spo11-HA3His6*/*spo11-HA3His6*	pKK11 (2μ *REC102*)	<0.5[b] (50)
SKY348	*REC102-myc9*/+, *spo11-HA3His6*/*spo11-HA3His6*	—	<1.25[b] (20)
SKY284	*REC102-myc9*/+, *spo11-HA3His6*/+	—	96 (50)

[a] The numbers of four-spored asci dissected are indicated in parentheses.
[b] No viable spores were recovered.

gous for either *REC102-myc9*/*REC102-myc9* or *spo11-HA3His6*/*spo11-HA3His6* yielded 97% viable spores, similar to wild type (Table 2). *REC102*- and *SPO11*-dependent recombination is essential for accurate meiotic chromosome segregation and therefore for production of viable spores. Thus, both tagged proteins could support initiation of meiotic recombination at a temperature commonly used for sporulation of laboratory strains.

Surprisingly, a diploid strain homozygous for both tagged alleles (SKY291) showed a modest but significant reduction in spore viability at 30° (78%, $P < 0.01$). To characterize this defect in more detail, we examined meiotic products produced at various temperatures. When these strains were sporulated at 37°, sporulation efficiency in all of them was reduced (data not shown), but those cells that were able to form tetrads yielded viable spores at similar frequencies as at 30°, with a modest reduction in viability in the doubly tagged strain relative to the others. However, when the sporulation temperature was lowered, the *spo11-HA3His6*/*spo11-HA3His6* strain manifested a mild cold-sensitive defect, with production of viable spores reduced to 59% at 16° (significantly different from wild type at $P < 0.01$). Notably, normal spore viabilities were observed at 16° in a strain homozygous for *SPO11-HA*, a version of *SPO11* used in earlier studies (Keeney *et al.* 1997; Cha *et al.* 2000).

The *REC102-myc9* allele supported wild-type spore viability by itself at reduced temperatures, but when both tagged constructs were combined in the same strain, a severe synthetic cold-sensitive phenotype was observed, with spore viabilities reduced to 7% and <1% after sporulation at 23° and 16°, respectively (Table 2). This synthetic phenotype indicates that the tagged *REC102* allele is not completely normal and that the defects associated with tagging both proteins act synergistically.

To confirm that the synthetic cold-sensitive phenotype was caused by the tagged alleles and not by an unlinked mutation(s), we reintroduced the wild-type *SPO11* gene on an *ARS-CEN* plasmid. Spore viability in the doubly tagged strain carrying a *SPO11* plasmid increased to 71% at 16° (Table 3). In contrast, introduction of a plasmid carrying the *spo11-HA3His6* allele did not rescue the spore viability defect. The partial rescue of the cold sensitivity by wild-type *SPO11* may reflect differences in expression due to allele copy number, because a *REC102-myc9*/*REC102-myc9 spo11-HA3His6*/*SPO11* strain showed wild-type spore viability (SKY540, Table 3), indicating that *spo11-HA3His6* is recessive to wild-type *SPO11* in single copy. Similarly, a double heterozygote showed no apparent defect at 16° (SKY284, Table 3).

When the same experiment was performed for *REC102-myc9*, neither an *ARS/CEN* plasmid (pKK9) nor a 2μ plasmid (pKK11) carrying the wild-type *REC102* allele was able to rescue the spore viability defect in the doubly tagged strain (Table 3). One explanation for these findings is that the *REC102-myc9* allele is dominant for the synthetic phenotype. In support of this hypothesis, a *REC102-myc9*/*REC102 spo11-HA3His6*/*spo11-HA3His6* strain yielded no viable spores from 20 tetrads formed at 16° (SKY348, Table 3), indistinguishable from the doubly tagged homo-

TABLE 4

Intragenic recombination frequencies at *his4LEU2*

Strain	Relevant genotype	*HIS4* recombinants per viable cell ($\times 10^3$)[a]		
			Meiotic[c]	
		Premeiotic[b]	16°	30°
SKY490	Wild type	0.13 ± 0.036	12.7 ± 3.2	14.7 ± 5.2
SKY10	*spo11Δ* / *spo11Δ*	0.019 ± 0.011	0.019 ± 0.015	
SKY493	*REC102-myc9* / *REC102-myc9*	0.12 ± 0.050	27.2 ± 10.8	10.2 ± 4.1
SKY496	*SPO11-HA3His6* / *SPO11-HA3His6*	0.075 ± 0.055	7.1 ± 5.2	8.0 ± 0.75
SKY470	*REC102-myc9* / *REC102-myc9*, *SPO11-HA3His6* / *SPO11-HA3His6*	0.041 ± 0.010	0.25 ± 0.18	3.6 ± 1.1

[a] Numbers are the average ± standard deviation of at least three determinations, except SKY10 at 16° (two determinations).
[b] Premeiotic samples were plated immediately after transfer to sporulation conditions.
[c] Samples were plated after 8 hr (30°) or 13 hr (16°) in sporulation conditions.

zygote (SKY291, Table 2). The alternative possibility that there is an unlinked sporulation mutation in the strain appears not to be the case, for two reasons. First, the same synthetic phenotype was observed in two independently generated strains carrying different *REC102-myc9* constructs, one marked with *URA3* (SKY291, Table 1) and the other with *TRP1* (data not shown). Second, the synthetic phenotype cosegregated with *REC102-myc9* when tetrads from a *REC102-myc9/REC102 spo11-HA3His6/spo11-HA3 His6* strain were dissected at 30° (data not shown).

Effects on initiation of meiotic recombination: Spore inviability can be caused by defects in any of a number of processes, not just meiotic recombination (Kupiec *et al.* 1997). To determine whether the genetic interaction between the tagged *SPO11* and *REC102* alleles specifically affected initiation of meiotic recombination, we measured intragenic recombination and DSB formation during meiosis. The frequency of recombination was measured in strains carrying heteroalleles within an artificial meiotic recombination hotspot, *his4::LEU2* (Cao *et al.* 1990). During meiosis in wild type, the frequency of His+ prototrophs increased by roughly two orders of magnitude over the spontaneous (premeiotic) level (SKY490, Table 4). Similar meiosis-specific levels were seen at 30° as at 16°, although the prototroph frequency was reproducibly lower at 16°. The *REC102-myc9/REC102-myc9* strain showed no significant decrease in recombination frequency relative to wild type, consistent with its high spore viability (SKY 493, Table 4). In fact, this strain reproducibly yielded approximately twofold more recombinants than its wild-type counterpart at 16°. The reason for this temperature-specific hyperrecombination phenotype is not currently known. Recombinant frequencies were slightly reduced in a *spo11-HA3His6/spo11-HA3His6* strain relative to wild type at 30° and 16° (SKY496, Table 4) and were also reduced in the doubly tagged strain at 30° (SKY470, Table 4). In contrast, meiotic recombinant frequencies were only ~2% of normal in the doubly tagged strain at 16° (SKY470, Table 4), consistent with the severe spore viability defect at this temperature.

DSBs at a hotspot near *THR4* on chromosome III (Goldway *et al.* 1993) were analyzed over meiotic time courses at 30° and 16°. With the restriction enzyme and probe combination used in these experiments, two prominent DSB sites are observed in this region (Figure 1A). As expected, DSBs appeared transiently at these sites in a wild-type strain at 30° (Figure 1B). Similar DSB levels were observed at these sites in singly and doubly tagged strains, and the breaks appeared and disappeared with kinetics roughly similar to wild type (Figure 1B and data not shown). At 16°, DSBs appeared at the same sites in wild type, but they appeared later and persisted longer than at 30° (Figure 1C and data not shown). At 16°, a *REC102-myc9/REC102-myc9* strain showed similar DSB levels and kinetics as wild type (Figure 1C), consistent with its spore viability and intragenic recombination frequency at *his4::LEU2*. In contrast, DSBs occurred at reduced levels at 16° in the *spo11-HA3His6/spo11-HA3His6* strain (~20% of wild type) and were not detected in the doubly tagged strain (Figure 1C). Thus, initiation of recombination at reduced temperature was affected by the tag on Spo11p and by the synergistic effect of combining the two tagged alleles.

Kinetics of binucleate formation: A subset of DSB-

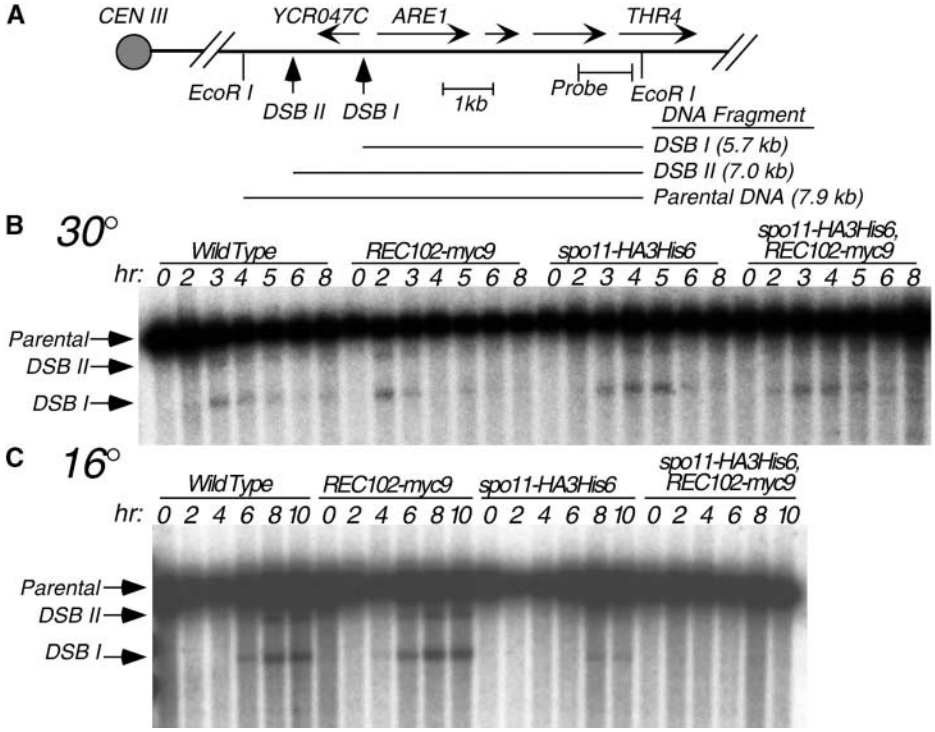

FIGURE 1.—Defects in meiotic DSB formation. (A) Schematic of the DSB hotspots near *THR4* on chromosome III (GOLDWAY *et al.* 1993). Horizontal arrows indicate ORFs. (B and C) Genomic DNA was prepared from synchronous meiotic cultures at the indicated times after transfer to sporulation conditions at 30° (B) or 16° (C) and analyzed by Southern blotting for the occurrence of DSBs. Early time points (prior to the disappearance of DSBs) are shown for the 16° culture to emphasize the time when DSBs are normally formed at this temperature. The strains used were NKY611 (wild type), SKY212 (*REC102-myc9/REC102-myc9*), SKY223 (*spo11-HA3His6/spo11-HA3His6*), and SKY291 (*REC102-myc9/REC102-myc9 spo11-HA3His6/spo11-HA3His6*).

defective mutants, including *spo11/spo11* and *rec102/rec102* nulls, have been reported to form binucleates earlier than normal, apparently carrying out the first meiotic division early (KLAPHOLZ *et al.* 1985; GIROUX *et al.* 1993; GALBRAITH *et al.* 1997; JIAO *et al.* 1999; CHA *et al.* 2000; SHONN *et al.* 2000). The basis of this phenomenon is not yet understood. To determine if the synthetic cold-sensitive defect conferred by the tagged *SPO11* and *REC102* alleles affected the timing of chromosome segregation, we analyzed binucleate and tetranucleate formation in meiotic time courses. Figure 2 contains cumulative curves showing accumulation of cells with two or more DAPI-staining bodies for wild-type, single-tagged, double-tagged, and *spo11* null mutant strains at 30° and 16°.

As expected from earlier studies in several strain backgrounds, including the SK1 background used here (KLAPHOLZ *et al.* 1985; GIROUX *et al.* 1993; CHA *et al.* 2000; SHONN *et al.* 2000), a *spo11*Δ*/spo11*Δ mutant formed binucleates significantly earlier than a wild-type control (Figure 2A). Under these conditions, 50% of the wild-type cells that were capable of carrying out any meiotic divisions had divided by 6–7 hr. In contrast, 50% of division-competent *spo11*Δ*/spo11*Δ mutant cells had already divided by 4 hr. At 16°, meiotic prophase was significantly extended, with ~19 hr required for 50% of wild-type cells to complete the first division (Figure 2B). Similar to the situation at 30°, the *spo11*Δ*/spo11*Δ strain carried out the first division significantly earlier than wild type at 16° (~13 hr).

At 30°, all of the single- and double-tagged strains showed division kinetics similar to wild type (Figure 2A). At 16°, in contrast, the doubly tagged strain divided much earlier than wild type, with similar kinetics to the *spo11*Δ*/spo11*Δ strain (50% with two or more nuclei by ~13 hr; Figure 2B). The *REC102-myc9/REC102-myc9* strain showed essentially wild-type division kinetics (21 hr for 50% of the cells to divide), but the *spo11-HA3His6/spo11-HA3His6* strain showed intermediate kinetics (~16–17 hr)—faster than wild type but slower than the *spo11*Δ*/spo11*Δ or doubly tagged strains.

The recombination defect in the doubly tagged strain is not caused by reduced steady-state protein levels: To determine whether these phenotypes reflected altered steady-state levels of Spo11-HA3His6p or Rec102-myc9p, we looked at protein expression by Western blotting with antibodies specific for the epitope tags. The anti-myc monoclonal antibody recognizes a protein with an apparent molecular mass of 50 kD in denaturing extracts of meiotic *REC102-myc9/REC102-myc9* cells, but not in control extracts from an untagged strain (Figure 3A). The mobility of this band is somewhat slow compared to the expected size of Rec102-myc9p (34 kD). The anti-HA antibody used in this study cross-reacts with an unidentified protein(s) in extracts from untagged control strains (asterisk in Figure 3A). This cross-reacting material migrates slightly slower than Spo11-HA3His6p, which migrates with an apparent molecular mass of 54 kD, in good agreement with its predicted size (50.5 kD).

Steady-state levels of Rec102-myc9p were assessed over meiotic time courses at 30° and 16° (Figure 3B). As expected from published studies of *REC102* mRNA expression (COOL and MALONE 1992), Rec102-myc9p was not detected in extracts from premeiotic cells. At 30°, Rec102-myc9p was detectable 1 hr after transfer to sporulation medium, it increased to a maximum by ~3 hr, and it

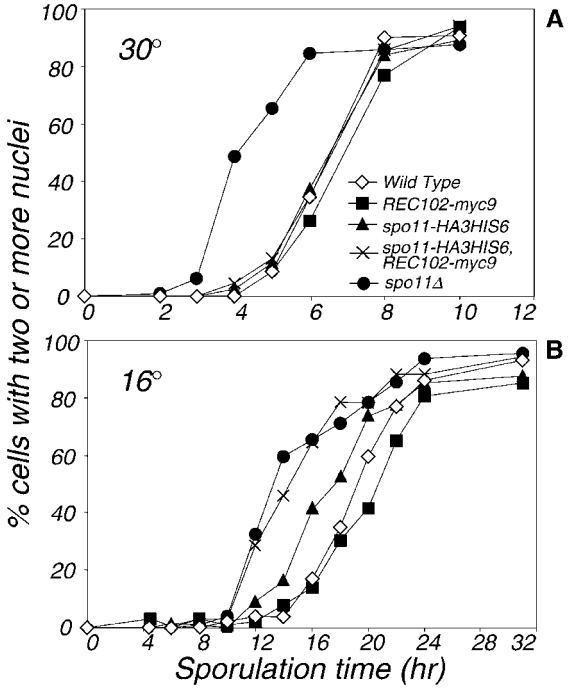

FIGURE 2.—Kinetics of the first nuclear division. Cells from synchronous meiotic cultures at the indicated temperatures were fixed and stained with DAPI at various times after transfer to sporulation conditions, and then the relative abundance of cells with one, two, or four nuclei was assessed. The plots show the percentage of cells that had formed two or more DAPI-staining bodies. At least 100 cells were counted for each time point. Strains were the same as in Figure 1, plus SKY10 (*spo11*Δ/*spo11*Δ).

persisted until at least 8 hr. A similar pattern was observed at 16°, except that appearance and accumulation to maximal levels were delayed relative to the 30° culture, as expected. We observed similar maximal protein levels at both temperatures. More importantly, both the kinetics of accumulation and the maximal Rec102-myc9p levels were indistinguishable when a *REC102-myc9/REC102-myc9* strain was compared to a *REC102-myc9/REC102-myc9 spo11-HA3His6/spo11-HA3His6* strain at either temperature. Thus, the recombination defect that we observed specifically in the doubly tagged strain at 16° cannot be attributed to differences in the steady-state level of Rec102-myc9 protein.

Levels of Spo11-HA3His6p in meiotic whole-cell extracts were also assessed (Figure 3C). Like Rec102-myc9p, Spo11-HA3His6p was not detected in extracts of premeiotic cells, as expected from documented mRNA expression patterns [ATCHESON *et al.* 1987; note that the tag-independent cross-reacting species (asterisk) is present in these samples]. At 30°, Spo11-HA3His6p was detected at 2 hr after transfer to sporulation medium, reached maximal levels by 3–4 hr, and persisted until at least 8 hr. At 16°, Spo11-HA3His6p was not detectable until ~6 hr and levels decreased again after ~10 hr. The maximal steady-state level reached was significantly lower than at 30°; this difference may contribute to the partial recombination defect observed in a *spo11-HA3His6/spo11-HA3His6* strain at 16° (above). However, extracts from a doubly tagged *REC102-myc9/REC102-myc9 spo11-HA3His6/spo11-HA3His6* strain were indistinguishable from the singly tagged *spo11-HA3His6/spo11-HA3His6* strain at this temperature. Therefore, the severe synthetic recombination defect in the doubly tagged strain at 16° is not caused by a further reduction in steady-state Spo11p levels.

Co-immunoprecipitation of Spo11p and Rec102p: The above observations establish a genetic interaction between *REC102* and *SPO11*. An immunoprecipitation analysis was carried out to determine if the products of these genes interact physically as well. Nondenaturing whole-cell extracts were prepared from *REC102-myc9/REC102-myc9* and *REC102/REC102* strains carrying *spo11-HA3His6*

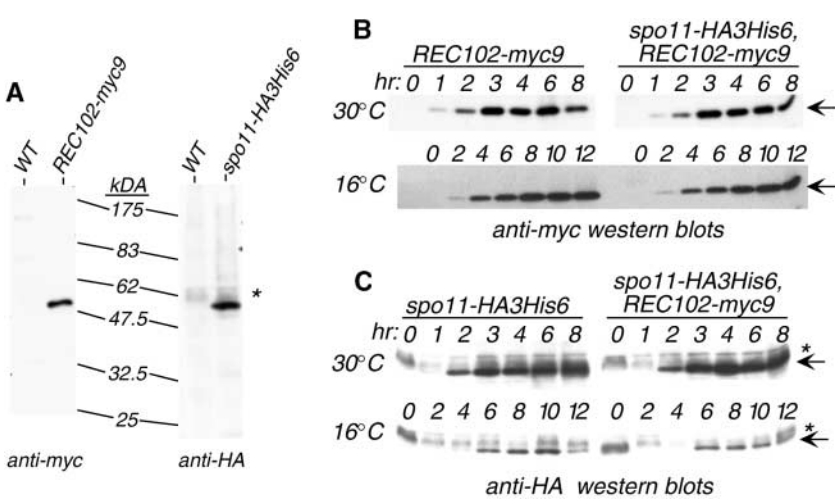

FIGURE 3.—Steady-state levels of Rec102-myc9p and Spo11-HA3His6p during meiosis. (A) Specificity of detection for the tagged proteins. Denaturing whole-cell extracts were prepared from meiotic cultures (4 hr at 30°) of strains homozygous for the indicated tagged constructs and from a wild-type control. Equal cell equivalents of extract were analyzed by Western blotting with anti-myc or anti-HA antibodies, as indicated. (B) Time course of Rec102-myc9p expression. Extracts were prepared at the indicated times after transfer to sporulation medium at 16° or 30° and analyzed by Western blotting with an anti-myc antibody. Arrows indicate the position of Rec102-myc9p. (C) Time course of Spo11-HA3His6p expression. The asterisks in A and C mark the position of tag-independent material that cross-reacts with the anti-HA monoclonal antibody. Arrows in B and C mark the positions of Rec102-myc9p and Spo11-HA3His6p, respectively. Strains were the same as in Figure 1.

3 hr after transfer to sporulation medium at 30°. Lysates were pretreated with DNase I to eliminate indirect binding of individual proteins via DNA and then immunoprecipitated with an anti-myc antibody (Figure 4A). Rec102-myc9p was efficiently depleted from the extract under these conditions (compare lanes 2 and 4) and was recovered in the eluate from the antibody matrix. (Although precipitation of Rec102-myc9p from the extracts was quantitative, the final recovery of the protein was inefficient, in part because mild elution conditions were used to prevent elution of immunoglobulin heavy chain, which comigrated with Rec102-myc9p on SDS-PAGE.) Spo11-HA3 His6p was depleted from the soluble fraction by 50–75% in the strain expressing Rec102-myc9p (compare lanes 2 and 4), relative to the control strain expressing untagged Rec102p (lane 3). Correspondingly, Spo11-HA3 His6p was specifically enriched in the immunoprecipitate from the *REC102-myc9/REC102-myc9* strain relative to the *REC102/REC102* strain (compare lanes 5 and 6). These results suggest that Rec102-myc9p and Spo11-HA3 His6p are components of a common protein complex *in vivo*. However, some of the Spo11-HA3His6 protein remained in the soluble fraction after the immunodepletion step even though all of the Rec102-myc9p was removed, perhaps indicating that not all Spo11 protein is contained in this putative multiprotein complex. We obtained similar results when lysates were prepared from cells sporulated at 16° (data not shown), suggesting that the synthetic recombination defect in the doubly tagged strain is not caused by a failure to incorporate these two proteins into the same complex.

To address the concern that this observed physical interaction was an artifact caused by the epitope tags themselves, we replaced the myc tag on Rec102p with three copies of the Flag epitope tag. Spo11-HA3His6p also coimmunoprecipitated with this version of Rec102p (Figure 4B), indicating that the interaction is not specific to the myc and HA tag combination. However, *REC102-Flag3* showed a synthetic cold-sensitive phenotype when combined with *spo11-HA3His6*, similar to that observed with *REC102-myc9* (Table 2). We therefore also tested whether Spo11p and Rec102p could interact in a strain in which there was no detectable recombination defect, namely in a *REC102-myc9/REC102-myc9* strain in which Spo11p was untagged. In this strain, untagged Spo11p specifically coprecipitated with Rec102-myc9p (Figure 4C). This result indicates that the observed physical interaction is independent of any cold-sensitive defect in recombination.

To date, we have been unable to efficiently precipitate Spo11p under nondenaturing conditions, using either antitag or polyclonal anti-Spo11p antibodies, even though Spo11p can be precipitated under denaturing conditions (data not shown). This may indicate that Spo11p epitopes are masked by the binding of other proteins in nondenaturing extracts.

Rec102-myc9p is a nuclear protein that associates with meiotic chromatin: We examined the subcellular distribution of Rec102-myc9p by indirect immunofluorescence on fixed, whole cells. Under the conditions of these experiments, the anti-myc antibody produced a faint labeling pattern over the cytoplasm of *REC102/REC102* control cells but did not specifically label the nuclei (Figure 5, C and D). In contrast, the antibody strongly labeled the nuclei of meiotic cells expressing Rec102-myc9p (Figure 5, A and B). Anti-myc antibody failed to label nuclei in a small proportion of cells (see example in Figure 5A). These appear to be cells that failed to enter meiosis, on the basis of double staining with anti-myc and anti-Red1p antibodies (data not shown). Nuclear labeling was not observed for premeiotic cells or if the anti-myc primary antibody was omitted (data not shown). We conclude that Rec102-myc9p localizes predominantly, if not exclusively, to the nucleus.

We also examined Rec102-myc9p localization on surface-spread meiotic chromosomes. The anti-myc antibody produced a punctate labeling pattern on chromosomes from meiotic cells expressing Rec102-myc9p (Figure 5,

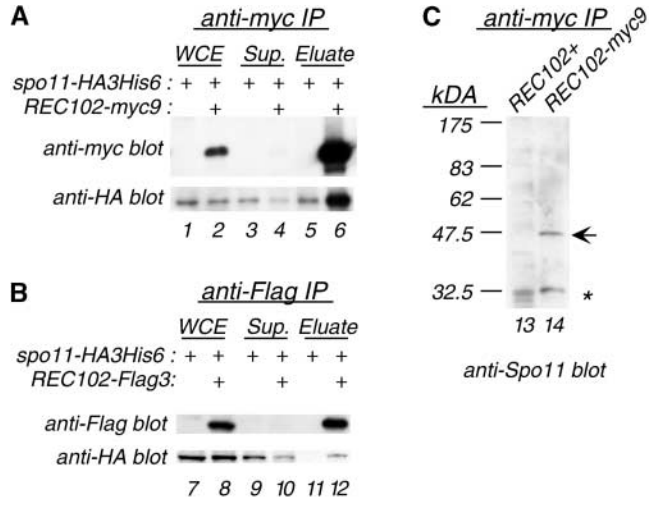

FIGURE 4.—Co-immunoprecipitation of Spo11p with Rec102-myc9p or Rec102-Flag3p. (A) Nondenaturing whole-cell extracts (WCE) were prepared from meiotic cultures of SKY223 (*spo11-HA3His6/spo11-HA3His6*) and SKY291 (*REC102-myc9/REC102-myc9 spo11-HA3His6/spo11-HA3His6*) and immunoprecipitated with an anti-myc monoclonal antibody. Rec102-myc9p and Spo11-HA3His6p were detected by Western blotting of equal cell equivalents of WCE and the immunoprecipitation supernatant (Sup.) and ~200 equivalents of the eluate from the affinity matrix. (B) Nondenaturing extracts prepared from SKY223 and SKY571 (*REC102-Flag3/REC102-Flag3 spo11-HA3His6/spo11-HA3His6*) were immunoprecipitated with an anti-Flag monoclonal antibody. Western blotting was performed on equal cell equivalents of WCE and supernatant and ~20 equivalents of the eluate from the immunoprecipitate. (C) Nondenaturing extracts prepared from a chromatin-enriched fraction from NKY611 (*REC102/REC102 SPO11/SPO11*) and SKY212 (*REC102-myc9p/REC102-myc9p SPO11/SPO11*) were immunoprecipitated with an anti-myc monoclonal antibody, and the precipitated proteins were analyzed by Western blotting with affinity-purified anti-Spo11p polyclonal antibodies. The arrow indicates the position of Spo11p; the asterisk indicates nonspecific cross-reacting bands.

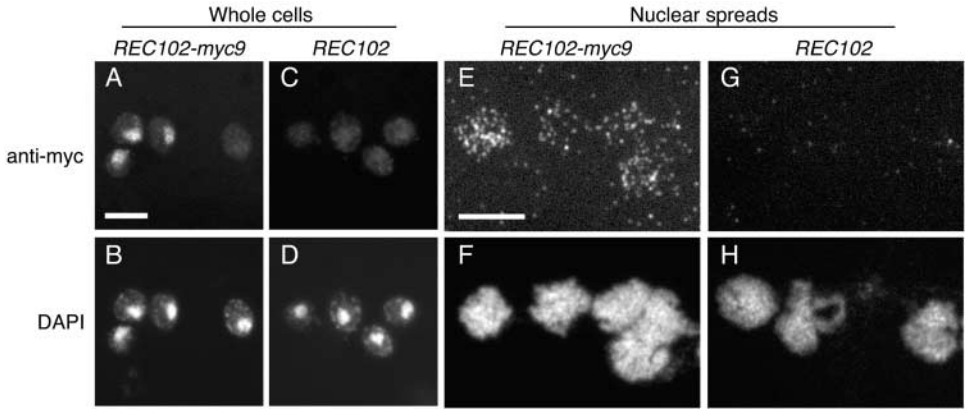

FIGURE 5.—Subcellular distribution of Rec102-myc9p. Fixed whole cells (A–D) or spread chromosomes (E–H) from synchronous meiotic cultures (4 hr at 30°) of SKY212 (*REC102-myc9/REC102-myc9*: A, B, E, and F) or NKY611 (wild type: C, D, G, and H) were immunostained with anti-myc antibody (A, C, E, and G) and stained with DAPI (B, D, F, and H). Bars: A–D, 5 μm; E–H, 5 μm.

E and F), but only a faint background pattern on chromosomes from an untagged control strain (Figure 5, G and H). No labeling was observed on spread nuclei from premeiotic cells or if the primary antibody was omitted (data not shown). Unfortunately, we have been unable to detect Spo11-HA3His6p on meiotic chromosomes using standard spreading and immunofluorescence techniques, so we have been unable to assess whether Rec102p and Spo11p localize to the same sites.

DISCUSSION

We report here a genetic interaction between *SPO11* and *REC102*, manifested as a synthetic cold-sensitive defect caused by combining epitope-tagged alleles of each gene in the same strain. While this work was in progress, we became aware that Giroux and colleagues had found that overexpression of *REC102* could partially suppress recombination defects conferred by temperature-sensitive *spo11* alleles (RIEGER 1999), providing further evidence for genetic interactions between these genes during DSB formation.

At least a fraction of tagged or untagged Spo11p coimmunoprecipitated with Rec102-myc9p and Rec102-Flag3p from soluble extracts of meiotic cells. We favor the interpretation that this coprecipitation reflects a physical association intrinsic to Spo11p and Rec102p, but we cannot fully exclude the formal possibility that the presence of any tag on Rec102p fortuitously creates an interaction with Spo11p that otherwise would not exist. Importantly, however, the observation that untagged Spo11p also associates with Rec102-myc9p (*i.e.*, in a strain with no detectable recombination defect) rules out any scenario in which an artifactual association between these proteins caused by epitope tagging in turn causes the observed cold-sensitive recombination defect.

Because of the genetic complexity of DSB formation, it is attractive to think that Spo11p-mediated breaks are formed within the context of a multiprotein complex assembled on meiotic chromosomes. Our results suggest that Rec102p is a component of this complex. Consistent with this interpretation, we show that Rec102p is a nuclear protein that localizes to meiotic chromosomes. To date, we have not been able to detect a direct interaction between Spo11p and Rec102p by yeast two-hybrid analysis or by immunoprecipitation of proteins cotranslated *in vitro* in rabbit reticulocyte extracts (our unpublished results). It is possible that Spo11p and Rec102p interact indirectly by associating with additional protein(s) or that they require a meiosis-specific post-translational modification to interact with one another. Recent studies identifying genetic interactions between *REC104* and *REC102* (SALEM *et al.* 1999), and between *REC104* and *SPO11* (RIEGER 1999), may indicate that Rec104p is also part of this putative multiprotein DSB complex.

Defects associated with epitope tags: Our results indicate that neither Spo11-HA3His6p nor Rec102-myc9p functions completely normally *in vivo*. There are many other examples in the literature of defects caused by epitope tags in yeast. For example, epitope tags at the carboxyl termini of Hrt1p or Apc11p conferred temperature-sensitive phenotypes (SEOL *et al.* 1999). However, our results suggest that even tagged alleles that appear to be fully functional by themselves (*i.e.*, *REC102-myc9*) may have subtle defects that are revealed only in a sensitized system.

The molecular basis of the *SPO11-REC102* genetic interaction remains to be determined. The synthetic cold sensitivity of DSB formation in a *REC102-myc9/REC102-myc9 spo11-HA3His6/spo11-HA3His6* strain is not due to changes in the steady-state level of either gene product or to defects in the incorporation of either protein into a common multiprotein complex at a restrictive temperature. One possible explanation for the observed defects could be that the tags interfere sterically with the binding of another factor(s) to the Spo11p-Rec102p complex. The cold sensitivity associated with *spo11-HA3His6* and with the synthetic interaction with *REC102* may indicate that Spo11p function is sensitive to perturbations in the assembly or disassembly of higher order protein-protein complexes.

Kinetics of chromosome segregation: A number of DSB-defective mutants in yeast, including *spo11*Δ and *rec102*Δ, appear to carry out the first meiotic division earlier than wild type on the basis of kinetics with which

two or more DAPI-staining bodies appear (Klapholz *et al.* 1985; Giroux *et al.* 1993; Galbraith *et al.* 1997; Jiao *et al.* 1999; Cha *et al.* 2000). For Spo11p, this phenotype is closely tied to its DSB-forming activity, because point mutations that alter putative active site residues (*e.g.*, *spo11-Y135F*) are indistinguishable from deletion mutants in this respect (Cha *et al.* 2000; R. Diaz and S. Keeney, unpublished results). One interpretation of this finding is that the early divisions represent early onset of anaphase, meaning that the length of prophase I is shortened in the mutants.

Murray and colleagues suggested an alternative interpretation on the basis of their observation that *spo11/spo11* mutants segregate their chromosomes prior to the onset of a true anaphase I stage (defined by degradation of the Pds1 protein; Shonn *et al.* 2000). It was proposed that achiasmate chromosomes are unable to resist the tension imposed by the prometaphase spindle, and thus chromosome masses are segregated concomitant with spindle assembly rather than upon entry into anaphase (Shonn *et al.* 2000).

This idea does not seem adequate to explain all of the available data, however, because *mei4/mei4* mutants, which like *spo11*Δ*/spo11*Δ also appear to be completely achiasmate, have normal division kinetics (Galbraith *et al.* 1997; Jiao *et al.* 1999). Moreover, we find that the partial recombination defect at 16° in a *spo11-HA3His6/spo11-HA3His6* strain correlates with an intermediate timing of chromosome segregation—earlier than wild type but not as early as a *spo11*Δ*/spo11*Δ strain (Figure 2). The simplest version of an "anaphase-like prometaphase" model does not predict such intermediate division timing in cases of partial recombination defects.

One possibility is that the timing of prometaphase spindle assembly is influenced by a subset of the gene products required for DSB formation, either directly or indirectly via feedback through the cell cycle machinery. Because *spo11/spo11* and *rec102/rec102* mutants form binucleates earlier than normal, these genes may be required to provide an inhibitory signal that normally delays spindle assembly, perhaps involving an altered chromatin or higher order chromosome structure (Jiao *et al.* 1999). Alternatively, a *mei4* mutation may cause a compensatory delay in prometaphase spindle assembly, such that the combined defects of a spindle delay and achiasmate chromosomes cause the mutant to mimic normal division timing. These ideas make testable predictions about the dynamics of spindle formation and elongation, chromosome segregation, and cell cycle progression (assessed by molecular markers such as Pds1p degradation) in the different mutants.

Kinetics of Spo11p and Rec102p accumulation: In comparing the timing of events of meiotic prophase (specifically, DSB formation and chromosome segregation) with steady-state protein levels, it is clear that Spo11-HA3 His6p continues to accumulate past the time when it is active in DSB formation and that it persists long after the first meiotic division (compare Figures 1–3). Similar results were obtained for Rec102-myc9p. These results suggest that the amount and timing of DSBs in normal meiosis are not controlled by limitations on the amount of free Spo11p (or Rec102p). Also, these findings reinforce the conclusion that one cannot infer the time of Spo11p function in other organisms from the timing of maximal protein accumulation.

The manner in which meiotic cells control the time and location of Spo11p-mediated DSBs is not yet clear. Understanding this control requires that we understand the roles of the factors that interact with Spo11p. The identification of Rec102p as such a factor provides an important step in this analysis.

We thank Doug Bishop, Steve Gasior, Craig Giroux, Nancy Kleckner, Noel Lowndes, and Pamela Meluh for providing strains, plasmids, and/or protocols, and Ed Louis for advice on statistical analysis. We also thank Frédéric Baudat, Michael Lichten, and members of the laboratory for helpful discussions and comments on the manuscript. This work was supported by National Institutes of Health grant GM58673 and funds from the Society of Memorial Sloan-Kettering.

LITERATURE CITED

Alani, E., R. Padmore and N. Kleckner, 1990 Analysis of wild-type and *rad50* mutants of yeast suggests an intimate relationship between meiotic chromosome synapsis and recombination. Cell **61:** 419–436.

Atcheson, C. L., B. DiDomenico, S. Frackman, R. E. Esposito and R. T. Elder, 1987 Isolation, DNA sequence, and regulation of a meiosis-specific eukaryotic recombination gene. Proc. Natl. Acad. Sci. USA **84:** 8035–8039.

Baudat, F., and A. Nicolas, 1997 Clustering of meiotic double-strand breaks on yeast chromosome III. Proc. Natl. Acad. Sci. USA **94:** 5213–5218.

Baudat, F., K. Manova, J. P. Yuen, M. Jasin and S. Keeney, 2000 Chromosome synapsis defects and sexually dimorphic meiotic progression in mice lacking Spo11. Mol. Cell **6:** 989–998.

Bergerat, A., B. de Massy, D. Gadelle, P. C. Varoutas, A. Nicolas *et al.*, 1997 An atypical topoisomerase II from Archaea with implications for meiotic recombination. Nature **386:** 414–417.

Bhargava, J., J. Engebrecht and G. S. Roeder, 1992 The *rec102* mutant of yeast is defective in meiotic recombination and chromosome synapsis. Genetics **130:** 59–69.

Bishop, D. K., D. Park, L. Xu and N. Kleckner, 1992 *DMC1*: a meiosis-specific yeast homolog of E. coli *recA* required for recombination, synaptonemal complex formation, and cell cycle progression. Cell **69:** 439–456.

Bullard, S. A., S. Kim, A. M. Galbraith and R. E. Malone, 1996 Double strand breaks at the *HIS2* recombination hot spot in *Saccharomyces cerevisiae*. Proc. Natl. Acad. Sci. USA **93:** 13054–13059.

Cao, L., E. Alani and N. Kleckner, 1990 A pathway for generation and processing of double-strand breaks during meiotic recombination in *S. cerevisiae*. Cell **61:** 1089–1101.

Celerin, M., S. T. Merino, J. E. Stone, A. M. Menzie and M. E. Zolan, 2000 Multiple roles of Spo11 in meiotic chromosome behavior. EMBO J. **19:** 2739–2750.

Cha, R. S., B. M. Weiner, S. Keeney, J. Dekker and N. Kleckner, 2000 Progression of meiotic DNA replication is modulated by interchromosomal interaction proteins, negatively by Spo11p and positively by Rec8p. Genes Dev. **14:** 493–503.

Cool, M., and R. E. Malone, 1992 Molecular and genetic analysis of the yeast early meiotic recombination genes *REC102* and *REC107/MER2*. Mol. Cell. Biol. **12:** 1248–1256.

Dernburg, A. F., K. McDonald, G. Moulder, R. Barstead, M. Dresser *et al.*, 1998 Meiotic recombination in *C. elegans* initiates by a conserved mechanism and is dispensable for homologous chromosome synapsis. Cell **94:** 387–398.

Esposito, M. S., and R. E. Esposito, 1969 The genetic control of sporulation in *Saccharomyces*. I. The isolation of temperature-sensitive sporulation-deficient mutants. Genetics **61:** 79–89.

Galbraith, A. M., S. A. Bullard, K. Jiao, J. J. Nau and R. E. Malone, 1997 Recombination and the progression of meiosis in *Saccharomyces cerevisiae*. Genetics **146:** 481–489.

Gasior, S. L., A. K. Wong, Y. Kora, A. Shinohara and D. K. Bishop, 1998 Rad52 associates with RPA and functions with Rad55 and Rad57 to assemble meiotic recombination complexes. Genes Dev. **12:** 2208–2221.

Gietz, R. D., and R. A. Woods, 1998 Transformation of yeast by the lithium acetate/single-stranded carrier DNA/PEG method. Methods Microbiol. **26:** 53–66.

Giroux, C. N., M. E. Dresser and H. F. Tiano, 1989 Genetic control of chromosome synapsis in yeast meiosis. Genome **31:** 88–94.

Giroux, C. N., S. Misra, M. Modesti and J. Guerreiro, 1993 Decision points and the genetic control of meiosis, pp. 1–17 in *Meiosis II: Contemporary Approaches to the Study of Meiosis*, edited by F. P. Haseltine and S. Heyner. American Assoc. for the Advancement of Science, Washington.

Goldway, M., A. Sherman, D. Zenvirth, T. Arbel and G. Simchen, 1993 A short chromosomal region with major roles in yeast chromosome III meiotic disjunction, recombination and double strand breaks. Genetics **133:** 159–169.

Green, C. M., H. Erdjument-Bromage, P. Tempst and N. F. Lowndes, 2000 A novel Rad24 checkpoint protein complex closely related to replication factor C. Curr. Biol. **10:** 39–42.

Grelon, M., D. Vezon, G. Gendrot and G. Pelletier, 2001 *AtSPO11-1* is necessary for efficient meiotic recombination in plants. EMBO J. **20:** 589–600.

Haber, J. E., 1998 The many interfaces of Mre11. Cell **95:** 583–586.

Jiao, K., S. A. Bullard, L. Salem and R. E. Malone, 1999 Coordination of the initiation of recombination and the reductional division in meiosis in *Saccharomyces cerevisiae*. Genetics **152:** 117–128.

Kaiser, C., S. Michaelis and A. Mitchell, 1994 *Methods in Yeast Genetics*. Cold Spring Harbor Laboratory Press, Cold Spring Harbor, NY.

Kane, S., and R. Roth, 1974 Carbohydrate metabolism during ascospore development in yeast. J. Bacteriol. **118:** 8–14.

Ke, S. H., and E. L. Madison, 1997 Rapid and efficient site-directed mutagenesis by single-tube 'megaprimer' PCR method. Nucleic Acids Res. **25:** 3371–3372.

Keeney, S., 2001 Mechanism and control of meiotic recombination initiation. Curr. Top. Dev. Biol. **52:** 1–53.

Keeney, S., and N. Kleckner, 1995 Covalent protein-DNA complexes at the 5′ strand termini of meiosis-specific double-strand breaks in yeast. Proc. Natl. Acad. Sci. USA **92:** 11274–11278.

Keeney, S., C. N. Giroux and N. Kleckner, 1997 Meiosis-specific DNA double-strand breaks are catalyzed by Spo11, a member of a widely conserved protein family. Cell **88:** 375–384.

Klapholz, S., C. S. Waddell and R. E. Esposito, 1985 The role of the *SPO11* gene in meiotic recombination in yeast. Genetics **110:** 187–216.

Kupiec, M., B. Byers, R. E. Esposito and A. P. Mitchell, 1997 Meiosis and sporulation in *Saccharomyces cerevisiae*, pp. 889–1036 in *The Molecular and Cellular Biology of the Yeast Saccharomyces: Cell Cycle and Cell Biology*, edited by J. R. Pringle, J. R. Broach and E. W. Jones. Cold Spring Harbor Laboratory Press, Cold Spring Harbor, NY.

Lin, Y., and G. R. Smith, 1994 Transient, meiosis-induced expression of the *rec6* and *rec12* genes of *Schizosaccharomyces pombe*. Genetics **136:** 769–779.

Loidl, J., K. Nairz and F. Klein, 1991 Meiotic chromosome synapsis in a haploid yeast. Chromosoma **100:** 221–228.

Loidl, J., F. Klein and H. Scherthan, 1994 Homologous pairing is reduced but not abolished in asynaptic mutants of yeast. J. Cell Biol. **125:** 1191–1200.

Loidl, J., F. Klein and J. Engebrecht, 1998 Genetic and morphological approaches for the analysis of meiotic chromosomes in yeast. Methods Cell Biol. **53:** 257–285.

Mahadevaiah, S. K., J. M. A. Turner, F. Baudat, E. P. Rogakou, P. de Boer *et al.*, 2001 Recombinational DNA double strand breaks in mice precede synapsis. Nat. Genet. **27:** 271–276.

Malone, R. E., S. Bullard, M. Hermiston, R. Rieger, M. Cool *et al.*, 1991 Isolation of mutants defective in early steps of meiotic recombination in the yeast *Saccharomyces cerevisiae*. Genetics **128:** 79–88.

McKim, K. S., and A. Hayashi-Hagihara, 1998 *mei-W68* in *Drosophila melanogaster* encodes a Spo11 homolog: evidence that the mechanism for initiating meiotic recombination is conserved. Genes Dev. **12:** 2932–2942.

Moore, D. P., and T. L. Orr-Weaver, 1998 Chromosome segregation during meiosis: building an unambivalent bivalent. Curr. Top. Dev. Biol. **37:** 263–299.

Padmore, R., L. Cao and N. Kleckner, 1991 Temporal comparison of recombination and synaptonemal complex formation during meiosis in *S. cerevisiae*. Cell **66:** 1239–1256.

Paques, F., and J. E. Haber, 1999 Multiple pathways of recombination induced by double-strand breaks in *Saccharomyces cerevisiae*. Microbiol. Mol. Biol. Rev. **63:** 349–404.

Pringle, J. R., A. E. Adams, D. G. Drubin and B. K. Haarer, 1991 Immunofluorescence methods for yeast. Methods Enzymol. **194:** 565–602.

Rieger, D. K., 1999 *Molecular Analysis of an Early Meiotic Decision Point in Yeast*. Ph.D. thesis, Wayne State University, Detroit.

Romanienko, P. J., and R. D. Camerini-Otero, 2000 The mouse *Spo11* gene is required for meiotic chromosome synapsis. Mol. Cell **6:** 975–987.

Salem, L., N. Walter and R. Malone, 1999 Suppressor analysis of the *Saccharomyces cerevisiae* gene *REC104* reveals a genetic interaction with *REC102*. Genetics **151:** 1261–1272.

Seol, J. H., R. M. Feldman, W. Zachariae, A. Shevchenko, C. C. Correll *et al.*, 1999 Cdc53/cullin and the essential Hrt1 RING-H2 subunit of SCF define a ubiquitin ligase module that activates the E2 enzyme Cdc34. Genes Dev. **13:** 1614–1626.

Sherman, F., and H. Roman, 1963 Evidence for two types of allelic recombination in yeast. Genetics **48:** 255–261.

Shonn, M. A., R. McCarroll and A. W. Murray, 2000 Requirement of the spindle checkpoint for proper chromosome segregation in budding yeast meiosis. Science **289:** 300–303.

Sikorski, R. S., and P. Hieter, 1989 A system of shuttle vectors and yeast host strains designed for efficient manipulation of DNA in *Saccharomyces cerevisiae*. Genetics **122:** 19–27.

Smith, K. N., and A. Nicolas, 1998 Recombination at work for meiosis. Curr. Opin. Genet. Dev. **8:** 200–211.

Tyers, M., G. Tokiwa, R. Nash and B. Futcher, 1992 The Cln3-Cdc28 kinase complex of *S. cerevisiae* is regulated by proteolysis and phosphorylation. EMBO J. **11:** 1773–1784.

Wach, A., A. Brachat, C. Rebischung, S. Steiner, K. Pokorni *et al.*, 1998 PCR-based gene targeting in *Saccharomyces cerevisiae*. Methods Microbiol. **26:** 67–81.

Communicating editor: M. Lichten